In vitro Silencing of Acetyl-CoA Carboxylase beta *(ACACB)* Gene Reduces Cholesterol Synthesis in Knockdown Chicken Myoblast Cells

G. Sushma
College of veterinary Science, Hyderabad, India
P. Jaya Laxmi
PV Narasimha Rao Telangana Veterinary University: Sri PV Narasimha Rao Telangana State Veterinary University
S.T. Viroji Rao
PV Narasimha Rao Telangana Veterinary University: Sri PV Narasimha Rao Telangana State Veterinary University
R.M.V. Prasad
PV Narasimha Rao Telangana Veterinary University: Sri PV Narasimha Rao Telangana State Veterinary University
M. Kanakachari
Directorate of Poultry Research
Ch. Shiva Prasad
College of Veterinary Science, Korutla, Telangana, India
A. Rajendra Prasad
Directorate of Poultry Research
D. Divya
Directorate of Poultry Research
Tarun Kumar Bhattacharya (bhattacharyatk@gmail.com)
Directorate of Poultry Research https://orcid.org/0000-0003-4502-1852

Research Article

Keywords: Chicken, fatty acid metabolism, ACACB, shRNA, myoblast cell culture, gene silencing.

Posted Date: June 18th, 2021

DOI: https://doi.org/10.21203/rs.3.rs-502942/v1

Abstract

The poultry industry provides cost-effective, healthy, and protein-enriched food for the growing population and achieving the nutritional security to the country. Excessive abdominal and subcutaneous fat deposition is one of the major setbacks to the poultry industry that reduces carcass yield and feed efficiency. In chicken abdominal fat constitutes 20% of total body fat which make up 2–3% of live weight of the bird. In fatty acid metabolism, acetyl-CoA Carboxylase (ACC) is one of the key enzymes with two isoforms *i.e. ACACA* and *ACACB* each of which plays a different role. In chicken, *ACACB* is involved in the β-oxidation of fatty acids and thereby potentially regulating the quality of meat and egg. The RNAi strategy is widely used for silencing the target gene expression. In this study, we designed five shRNA constructs and identified the most efficient shRNA molecule for silencing the *ACACB* gene under *in vitro* chicken embryo myoblast (CEM) primary cell culture system. After knocking down the *ACACB* gene, for understanding how fatty acid metabolism is regulated, we tracked the expression of key fatty acid metabolism genes like *ACACA*, *FASN*, *SCD*, *ELOVL2*, and *CPT1*. Also, checked the expression of immune response genes like *IFNA*, *IFNB*, and *BLB1* in control as well as *ACACB* knockdown myoblast cells and observed no significant difference. We observed the down-regulation of key fatty acid metabolism genes along with *ACACB*, which may leads to the less fat accumulation in CEM cells. We also estimated the cholesterol and triglycerides in control and *ACACB* knockdown myoblast cells and found a significant difference between control and the knockdown cells. *In vitro* knockdown of the *ACACB* gene in a cell culture system by a short hairpin RNA (shRNA) expressing construct would help to produce a knockdown chicken with reduced fat deposition.

Introduction

The major objective of poultry production is to provide cheaper, safe, healthy, and protein-enriched food for the growing population thereby achieving the nutritional security to the country. Due to the adoption of improved nutritional strategies and technological innovations creating better rearing conditions, the poultry industry has grown greatly in recent years by making the chicken attaining a finishing body weight of about 2 kg in a very short period. On the contrary, apart from resulting in excessive body fat deposition, this rapid growth rate leads to the high incidence of metabolic diseases and skeletal disorders with increased mortality. In broiler chicken abdominal fat constitutes 20% of total body fat and excessive body fat has been recognized as a major problem in the poultry industry, which make up 2–3% of the total live weight of the broiler chicken (Cahaner et al. 1986; Butterwith 1989; Crespo and Esteve-Garcia 2002; Haro 2005; Leenstra 1986). Fat has limited value both to the poultry producer and consumer. Hence, excessive abdominal and subcutaneous fat deposition is one of the major setbacks to the poultry industry that reduces carcass yield, feed efficiency and ultimately causing consumers non-acceptance of meat (Lippens 2003; Jennen 2004). These negative viewpoints are of significant concern for the rancher and processor as they can bring considerable economic losses (Leenstra 1986; Pym 1987; Griffin 1996; Zubair and Leeson 1996; Buys et al. 1998; Buyse 1999; Havenstein et al. 2003; Nikolova et al. 2007). Moreover, in recent years, preference for leaner meat has been increasing as the consumers are becoming more sensitive about the positive correlation between intake of fatty substances and onset of cardiovascular diseases (Leeson and Summers 1980; Pym 1987; Cable and Waldroup 1990).

In avian species, major site of fat deposition, the abdominal fat pad is the prime indicator of total body fat content (Becker et al. 1979; Thomas et al. 1983). The fat deposition in body tissues is the net result of absorption, *de novo* synthesis, and β-oxidation of fatty acids (Saadoun and Leclercq 1986). As most of the traditional dietary approaches like restricted feeding techniques to combat excessive fattening in commercial broilers have resulted in decreased genetic potential for weight gain and failed in cost perspective, it would be more appropriate to emphasize the molecular regulation of fatty acid metabolism (Dunnington et al. 1986). In fatty acid metabolism, Acetyl-CoA Carboxylase (*ACC*) is the key enzyme with two isoforms, *ACACA* and *ACACB* each of which plays a different role concerning fat metabolism. The *ACACA* and *ACACB* catalyzes the carboxylation of acetyl-CoA to malonyl-CoA and malonyl-CoA generated via *ACACA* isoform mainly provides carbon units for fatty acid synthesis in lipogenic tissues like liver and adipose tissue whereas malonyl-CoA produced by *ACACB* isoform regulates fat oxidation by inhibiting carnitine palmitoyl transferase-1 (*CPT-1*), which controls the entry of long-chain fatty acids into the mitochondrial site of oxidation in nonlipogenic tissues like the heart and skeletal muscles (Abu-Elheiga 2000; Abu-Elheiga 2001). Hence, inhibition of *ACACB* may lead to reduced fat deposition by increasing fatty acid oxidation. Therefore, we

can reduce the expression of *ACACB* for improving poultry meat in terms of quality (leaner meat) as well as quantity (weight gain). Feeding experiments on mice revealed that, apart from consuming more food, *ACACB* knockout mice had lower body fat than their wild-type counterparts and were protected from high fat-induced obesity (Abu-Elheiga 2001; Abu-Elheiga et al. 2005; Oh et al. 2005; Abu-Elheiga et al. 2003). If we knockout the *ACACB* gene, it may result in deleterious or undesired outcomes, so RNAi-based gene knockdown provides a potential alternative to gene knockout technology. Transgenic RNAi mice showed a gene knockdown phenotype that was functionally similar to gene knockout (Hemann et al. 2003; Wang et al. 2010). Therefore, down-regulation of *ACACB* gene expression is a suitable approach to reduce the fat deposition by increased fatty acid oxidation. RNAi has been a standard method in both cultured cells and various model organisms for the controlled down-regulation of gene expression (Tripathi et al. 2012).

In chicken, Acetyl CoA carboxylase beta (*ACACB*) gene is involved in fatty acid metabolism and thereby, potentially regulating the quality of meat and egg. It is considered that *in vitro* knockdown of the *ACACB* gene in cell culture system by developing a short hairpin RNA (shRNA) expressing construct would help, in devising suitable *in vivo* strategies for knocking down of the gene. This, in turn, might help to produce a knockdown chicken with reduced fat deposition. The present investigation was designed with the objective of silencing *ACACB* gene with potential shRNA molecule and its effect on other fat synthesis genes under *in vitro* cell culture system.

Materials

Animals

The experiment was conducted in control broiler chicken line maintained at the Institute farm, ICAR-Directorate of Poultry Research, Hyderabad, India. The fertile eggs were collected from this chicken line and incubated in the incubator for 9 days at 98-100^{o}C with 78–80% relative humidity and turning 6 times a day for embryo development from which embryonic muscle tissues were collected for chicken embryo myoblast cell culture. The entire study was approved by the Institute Animal Ethics committee (IAEC) and Institute Bio-safety Committee (IBSC) of ICAR-Directorate of Poultry Research, Hyderabad, India. All the bio-safety guidelines of IBSC were followed while conducting the experiments.

Designing and cloning shRNA molecules

BLOCK-iT RNAi Designer (https://rnaidesigner.thermofisher.com/rnaiexpress/) is an online tool that was used to build five separate shRNA sequences that target the *ACACB* gene's open reading frame (ORF) using Tuschl's motif pattern. The siRNA sequences were then transformed into shRNA with CGAA as the stem-loop sequence and sense loop antisense as the strand orientation. The final shRNA has a 4-nucleotide 5' overhang (CACC or AAAA) for directional cloning of the ds oligos encoding the shRNA of interest (Table 1). The IDT manufacturers (Integrated DNA Technologies, USA) synthesized the oligos, and scrambled shRNA oligos (lac z) were supplied by the Invitrogen manufacturers (Invitrogen, USA) used in this experiment. The integrity of the ds oligos was checked by loading 5µl annealed ds oligo (500 nM stock) into 4% agarose gel. Both annealed ds oligos (50 bp) and remaining unannealed ss oligos (25 bp) were observed in the gel electrophoresis (Fig. 1). The annealed oligos were cloned into pENTR™/U6 vector (Invitrogen, USA) according to the manual instructions. The transformed recombinant colonies on LB agar plates were screened by using forward (U6: 5'-GGACTATCATATGCTTACCG-3') and reverse (M13: 5'-CAGGAA ACAGCTATGAC-3') primers for checking the presence or absence of shRNA inserts (Fig. 1). The plasmid obtained from each pENTR^{TM}/U6 entry construct was sequenced to confirm the sequence and orientation of the ds oligos insert.

Table 1
List of top and bottom strand sequences *ACACB* designed shRNA. Nucleotides in bold letters creates over hangs for cloning in the pENTR^{TM}/U6 vector.

shRNA ID	Nucleotide sequence (5' to 3')
Scrambled shRNA top	**CACC**GCTACACAAATCAGCGATTTCGAAAAATCGCTGATTTGTGTAG
Scrambled shRNA bottom	**AAAA**CTACACAAATCAGCGATTTTTCGAAATCGCTGATTTGTGTAGC
shRNA 1 top	**CACC**GGACAACTCCTCTGATGATGACGAATCATCATCAGAGGAGTTGTCC
shRNA 1 bottom	**AAAA**GGACAACTCCTCTGATGATGATTCGTCATCATCAGAGGAGTTGTCC
shRNA 2 top	**CACC**GCGATACTCCCATCTGCTTCACGAATGAAGCAGATGGGAGTATCGC
shRNA 2 bottom	**AAAA**GCGATACTCCCATCTGCTTCATTCGTGAAGCAGATGGGAGTATCGC
shRNA 3 top	**CACC**GCTGGTGACCATGTTAATTGACGAATCAATTAACATGGTCACCAGC
shRNA 3 bottom	**AAAA**GCTGGTGACCATGTTAATTGATTCGTCAATTAACATGGTCACCAGC
shRNA 4 top	**CACC**GCTCCGAAGAATCACGTTTCTCGAAAGAAACGTGATTCTTCGGAGC
shRNA 4 bottom	**AAAA**GCTCCGAAGAATCACGTTTCTTTCGAGAAACGTGATTCTTCGGAGC
shRNA 5 top	**CACC**GGACATCATTGGGAAGGATCACGAATGATCCTTCCCAATGATGTCC
shRNA 5 bottom	**AAAA**GGACATCATTGGGAAGGATCATTCGTGATCCTTCCCAATGATGTCC

Prediction of secondary structure and thermo dynamic properties of *ACACB* shRNA molecules

The RNA fold program of the Vienna RNA web service version 2.0 (http://rna.tbi.univie.ac.at/cgi-bin/RNAWebSuite/RNAfold.cgi) was used for the prediction of the secondary structures of all five shRNA molecules of chicken *ACACB* antisense and sense strands (Fig. S1). Further, secondary structures of chicken *ACACB* mRNA were predicted using a web server Mfold 2.3 version (http://www.unafold.org/mfold/applications/rna-folding-form-v2.php) (Fig. S2).

The Oligowalk software in the RNA structure version was used to determine the thermodynamic properties regulating each shRNA molecule's binding affinity to its mRNA target region were envisaged (http://rna.urmc.rochester.edu/cgi-bin/server_exe/oligowalk/ oligowalk_form.cgi) (Table 2). Hence, the following parameters were taken into account: $\Delta G_{overall}$ (Overall Gibbs free energy change): The net energy (ΔG in kcal/mol) resulting due to binding of oligos to the target site when all energy contributions are considered which includes target structure breaking energy and oligo self-structure energy. The more negative value of ΔG indicates a more stable duplex. ΔG_{duplex}: It measures the oligo target binding affinity. A more negative value of ΔG_{duplex} indicates more stability of the duplex and vice versa. $\Delta G_{break-target}$ (disruption energy): The energy cost for disrupting base pairs in mRNA target region so that the binding site becomes single-stranded and completely accessible. A more negative value denotes that the binding site is less accessible. $\Delta G_{intra-oligomer}$ and $\Delta G_{inter-oligomer}$: The negative ΔG of stable structures was greater than that of unstable structures. The free energy changes/differences caused by unimolecular and bimolecular siRNA foldings. $\Delta\Delta G_{ends}$: It tests the free energy variations in base pairing between the two ends of the antisense strands in the siRNA duplex, *i.e.* the 3' and 5' ends of the antisense strands, also known as differential stability of siRNA duplex ends (DSSE). The main characteristic of an effective siRNA is the unstable 5'end (End-diff is more positive).

Table 2
Sequence based parameters and thermodynamic parameters of shRNA molecules predicted by Oligo Walk algorithm.

S. No.	Nucleotide sequence of target region	Sequence based features			Thermodynamic features (kcal/mol)					
		Position on mRNA	Target Exon	GC%	Overall ΔG	Duplex ΔG	Break-target ΔG	Intra oligo ΔG	Inter oligo ΔG	End diff ΔG
1	GGACAACTCCTCTGATGATGA	267–287	1	47.60	-29.7	-34.2	-1.2	-1.0	-11.8	2.66
2	GCGATACTCCCATCTGCTTCA	1628–1648	11	52.30	-24.6	-31.1	-1.9	-1.9	-15.2	1.14
3	GCTGGTGACCATGTTAATTGA	3288–3308	23	42.85	-26.6	-32.1	-1.5	-1.1	-12.9	2.49
4	GCTCCGAAGAATCACGTTTCT	4113–4133	31	47.60	-26.5	-31.9	-1.7	-1.4	-14.2	2.27
5	GGACATCATTGGGAAGGATCA	5424–5444	40	47.60	-31.3	-33.9	-1.0	-0.1	-10.9	2.76

Chicken embryo myoblasts (CEM) primary cell culture

The 9-day old embryos were used for preparing the chicken embryo myoblast (CEM) primary cell culture (Sato et al. 2006). The collected eggs were cleaned with 70% ethanol and the broad end of the egg was cracked using sterile forceps and peeled off the white shell membrane to reveal the chorioallantoic membrane (CAM) below along with blood vessels. The sterile curved forceps were used for piercing the CAM and gently grasping the embryo under the head and lifted out, and transfer to the sterile 9-cm petri dish containing sterile phosphate buffer saline (PBS) and rinsed thoroughly. The head, limbs, and wings were removed by using scissors, and finally, the ventral side of the embryo was cut open to remove all internal organs and transferred in to a new second petri dish to dissect unwanted tissue like fat or necrotic material, debris and blood tinge was removed by washing with PBS several times. The sterile scissors were used to cut the tissue into fine 3-mm pieces. The minced tissue pieces were transferred to a sterile beaker containing a sterile magnetic bar and 10 ml of 2.5% trypsin, and the beaker was placed on the magnetic stirrer for stirring at about 100 rpm for less than 10 minutes at 37^0C and it was further filtered through a sterile double-layered muslin cloth into a fresh beaker and the filtrate was centrifuged for 5 minutes at 1500 rpm. After discarding the supernatant the resulting pellet was resuspended in 5 ml of growth medium (DMEM, HiMedia) with fetal bovine serum (FBS) to stop the trypsin action. The cell suspension was diluted to $1x10^6$ cells/ml in a growth medium with the help of a hemocytometer and seeded approximately $2x10^5$ cells/cm^2 in each 25-cm^2 tissue culture flask. The tissue culture flasks were incubated at 37^0C with 5% CO_2 until a confluent monolayer was obtained.

Transfection of shRNA construct

The recombinant shRNA clone (pENTR™/U6 Entry vector with respective shRNA insert) against *ACACB* gene and a control plasmid (plasmid containing scrambled shRNA) was transfected into the chicken embryo myoblast (CEM) primary cell culture using the Gene Pulser Xcell™ Electroporation system (Bio-Rad) to predict the activity of respective shRNAs in myoblasts. Two days before electroporation, the cells were transferred to a new 25-cm^2 tissue culture flask with fresh growth medium (DMEM) supplemented with 10% FBS and antibiotic antimycotic solution. The cells were grown up to the late-log phase, such that there will be 70–80% confluent on the day of the experiment. Adherent cells were first trypsinized by adding 0.1ml/cm^2 trypsin, it was finally inactivated with complete medium, and the cells were harvested by centrifuging at 1500 rpm for 5 minutes at room temperature. The cell pellet was re-suspended in growth medium yielding an approximate cell concentration of 2.5 X 10^6 cells/ml medium. The transfection reactions of all the shRNAs along with scrambled shRNA were carried out in triplicates. Approximately 0.4ml of the cell suspension was transferred into a 0.4 cm electroporation cuvette and the purified plasmid DNA was added to the cell suspension to a final concentration of approximately 50µg/ml. The DNA and cell suspension were mixed

in the cuvette and placed in the shock pod unit holder in the electroporation apparatus and a single square wave pulse was given at 110V with 25 milliseconds pulse length. After the pulse, cell suspension was transferred into a 25-cm^2 flask containing 5ml of growth medium. The flasks were rocked gently to assure even distribution of the cells over the surface of the flask and incubated at 37^0C in a CO_2 incubator. After 48 hours of transfection, the adherent cells were trypsinized and transferred into sterile 15ml conical tubes. The cells were harvested by centrifuging at 1000 rpm for 10 minutes and stored at -80^0C until total RNA isolation.

Total RNA isolation and cDNA synthesis

The total RNA was isolated from the CEM cell pellet using 1ml of Trizin (GCC Biotech, India), according to the manufacturer's protocol. After homogenization, the sample was incubated for 5 minutes at room temperature and then chloroform (200µl/sample) was added to the sample, shaken vigorously for 15 seconds, and incubated for 5 minutes at room temperature followed by centrifugation at 12000 rpm for 15 minutes at 4^0C. The upper aqueous phase was transferred to a new 1.5ml RNase free sterile microcentrifuge tube and 500µl of isopropanol was added for precipitation. The tubes were incubated for 30 minutes at -20^0C and then pelleted by centrifuge at 12000 rpm for 10 minutes at 4^0C. The pellet was washed with 750µl of 75% ethanol, air-dried the pellet for 5 to 10 minutes, and then dissolved in 20µl of RNase-free water. The total RNA was treated with DNase I (HiMedia, India) to remove any trace amount of genomic DNA. The RNA quality and quantity were checked by 1.2% denatured agarose gel and Jenway™ Genova Nano Micro-volume Spectrophotometer (Fisher Scientific, USA) respectively. For each sample, 2µg of total RNA was reverse transcribed using the Verso cDNA Synthesis Kit (Thermo Scientific, USA) in a 20µl reaction using Oligo dT and random primers. The cDNAs were diluted at 1:3 with nuclease-free water before the qPCR analysis.

Primer designing and qRT-PCR

A total of 9 genes were selected on the basis of their role in *de novo* fat synthesis and immune response *viz. ACACA* (Acetyl-CoA Carboxylase Alpha), *ACACB* (Acetyl-CoA Carboxylase Beta), *FASN* (Fatty acid synthase), *SCD* (Stearoyl-CoA Desaturase), *ELOVL2* (ELOVL Fatty Acid Elongase 2), *CPT1* (Carnitine palmitoyltransferase 1), *IFNA* (Interferon alpha), *IFNB* (Interferon Beta), and *BLB1* (Major histocompatibility complex class II beta chain *BLB1*). The sequences were downloaded from NCBI and CDS region was identified by using the ExPASy translation tool (https://web.expasy.org/translate/) and the primers were designed based on CDS using IDT Primer Quest software (https://www.idtdna.com/Primerquest/Home/Index) (Table 3). The expression levels of target genes (*ACACA*, *ACACB, FASN, SCD, ELOVL2, CPT1, IFNA, IFNB*, and *BLB1*) and reference gene Albumin (*ALB)* were quantified using thermal cycler Himedia Insta Q96™ with Bright Green 2X qPCR Master mix ROX (abm, Canada). The qPCR experiments were performed in a 10µl reaction volume [containing 1µl of diluted cDNA, 5µl of BrightGreen 2× qPCR MasterMix, 0.3µl of each primer] under the following program: an initial denaturation for 5 minutes at 95^0C, followed by 40 cycles of amplification with the 30s of denaturation at 95^0C and 60s of annealing/extension at 60^0C. The dissociation curve was obtained by heating the amplicon from 55 to 95^0C. All qPCR reactions were carried out in three biological replicates. Non-template controls (NTC) were also included in each run for each gene.

Table 3
The List of primers used for quantitative real-time PCR (qRT-PCR).

S. No.	Gene Symbol	Primer Sequences (5'-3')	Amplicon Size (bp)	Annealing temp (°C)	Accession No.
1	*ACACA*	F: CAGATTTGTTGTCATGGTGAC	162	60	NM_205505.1
		R: ACAGCCTGCACTGGAATGC			
2	*ACACB*	F: GCTCCTGCTGCCCATATATTA	94	60	NC_006102
		R: GTCCGTGATGACACCTTTCT			
3	*FASN*	F: GTTCTCTGTACAGAGAATGTG	168	60	NM_205155.3
		R: CCATGTTTGACTTGGTTGATC			
4	*SCD*	F: TGACGCTGATCCCTTCTGC	152	60	NM_204890.1
		R: AATAGTCAAGAAGATCCGCAG			
5	*ELOVL2*	F: ATGTTTGGACCTCGAGATGC	221	60	NM_001197308.1
		R: CACGTGGCAAGGATGAGC			
6	*CPT1*	F: GCCTTCGTGCGCAGTAT	146	60	DQ314726.1
		R: ACGTAGAGGCAGAAGAGGT			
7	*ALB*	F:TCCTGATCCGCTACACTAAGA	98	60	NM_205261.2
		R:CTGGCAGCACTTAGTACCAATA			
8	*IFNA*	F: CTGCTCACGCTCCTTCTG	170	60	NM_ 205427
		R: GTGTCGTTGAAGGAGCAAG			
9	*IFNB*	F: CTCCTTCAGAATACGGCTC	164	60	NM_ 001024836
		R: GTGTGTGGGCTGCTAAGC			
10	*BLB1*	F:TGAGTGCCACTACCTGAAC	200	60	NM_001044679
		R:GGCAGTACGTGTCCACTG			

Estimation of cholesterol and triglycerides

After forty-eight hours of transfection, control as well as *ACACB* knockdown adherent cells were trypsinized and transferred into 15ml sterile conical tubes and pelleted by centrifugation for 10 minutes at 10000 rpm. The pellet was washed with ice-cold PBS by centrifugation at 10000 rpm for 10 minutes at 4^0C. After harvesting of cells we counted the cell numbers from each culture flask in neubauer chamber and thus normalized the cell numbers before proceeding to estimate cholesterol and triglycerides. For each category (knockdown group and control group) equal number of cells ($1x10^6$ of cells/ml) were collected for estimation of cholesterol and triglycerides. The pellet was lysed by using 1ml complete cell extraction buffer (150 mM NaCl, 1% NP-40, 0.1% Sodium dodecyl sulphate, and 50 mM Tris, pH8) and the lysate was transferred to the 1.5ml sterile microcentrifuge tubes, vortexed the tubes and incubated on ice for 30 minutes with occasional vortexing. The lysate was centrifuged at 4^0C for 20 minutes at 14000 rpm and aqueous phase was collected into 1.5ml sterile microcentrifuge tubes. This cell extract was used for cholesterol and triglycerides estimation with the help of the Turbo Chem 100 automatic blood analyzer. The commercially available cholesterol and triglyceride reagent kits (Identi cholesterol test kit, Identi Triglyceride test kit CPC Diagnostics, Chennai, India) were used for cholesterol and triglycerides estimation.

Statistical analysis

The experiments were repeated twice, the relative expression of each gene was calculated by using $2^{-\Delta\Delta Ct}$, and statistical analysis was carried out using the trial version of SPSS 25. A univariate general linear model with Tukey's HSD and DMRT as post hoc test was used to study the significant difference between different shRNA groups due to the knockdown effect of target genes. Data from representative experiments were presented as Mean ± SE for different samples with differences determined by least significant differences at 5% level ($p \leq 0.05$).

Results

Secondary structures and thermodynamic properties for shRNAs

The evaluation of the shRNA constructs 1 and 5 were devoid of any secondary structures in their antisense strands while shRNA constructs 2, 3, and 4 formed secondary structures (Fig. S1). Hence, the shRNAs 1 and 5 showed minimum free energy (MFE) of 0.00 kcal/mol whereas, the shRNA 2, 3, and 4 showed MFE of -1.40, 0.30, and 0.10 kcal/mol respectively, due to the secondary structure formation (Fig. S1). The stem loop structures were formed for all the *ACACB* mRNA target regions of anti-*ACACB* shRNA molecules (Fig. S2). The GC percent of shRNAs ranged from 43–52% where shRNA 3 had the lowest (43%) of all the shRNAs studied, while shRNA 2 had a higher percentage (52%). The predicted values (negative) about overall/net ΔG value, ΔG duplex, and ΔG break-target were found to be highest in shRNA 5, shRNA 1, and shRNA 2 respectively, while the lowest values were observed in shRNA 2, shRNA 2, and shRNA 5, respectively. The DSSE was found to be highest for shRNA 5 and lowest for shRNA 2 (Table 2).

Cloning and confirmation of *ACACB* anti shRNA in pENTR™/U6 Vector

The RNAi-Ready pENTR™/U6 vector was used to ligate all the five shRNA oligos of the *ACACB* gene and transformed into One Shot TOP10 chemically competent *E. coli* cells. The recombinant clones of all the shRNAs were confirmed by colony PCR (Fig. 1). Further, the plasmid DNA was isolated from the recombinant clones and confirmed by plasmid PCR (Fig. 1). Each recombinant pENTR™/U6 construct was sequenced to confirm the sequence of the shRNA, which revealed the absence of mutations. The DNA was isolated from the transfected cell culture of each construct and used as a template in PCR to check for the presence of pENTR™/U6 Entry vector contains shRNA and found a product of 293 bp length signifying the successful transfection (Fig. 1).

Silencing efficiency of *ACACB* shRNAs

The qRT-PCR was performed with *ACACB* and *ALB* gene specific primers with all five shRNA treated CEM samples and scrambled shRNA treated samples was used as a control. The initiation phase, exponential phase, and plateau phase of amplification curves were all optimal, indicating that the product was amplified exponentially, i.e. fluorescence emission was corresponding to the amplified template. Melting curve analysis was performed at the end of the qRT-PCR cycle to verify the specificity of amplification, revealed a single peak for all genes, suggesting that the PCR products were homogeneous. The knockdown performance of shRNA 1 and 5 against scrambled shRNA was found to be significantly different ($P \leq 0.05$) in the qRT-PCR study. The fold change of *ACACB* gene in different shRNA constructs was 0.33, 0.75, 0.61, 0.62 and 0.31 in the cells with shRNA 1, shRNA 2, shRNA 3, shRNA 4 and shRNA 5 constructs respectively. In contrast to the scrambled shRNA, the knockdown (KD) percent of *ACACB* mRNA caused by different shRNA ranged from 69% (shRNA 5) to 25% (shRNA 2), respectively (Fig. 2).

Effect of shRNAs on immune response genes

In the knockdown cells, the relative expression of immune response genes such as *IFNA*, *IFNB*, and *BLB1* was also monitored by qRT-PCR in target as well as control samples. However, when compared with scrambled shRNA, no significant difference was observed in all five shRNA groups (Fig. 3).

Relative quantification of *de novo* fat synthetic genes

Once the knockdown of *ACACB* gene was found, the relative expression of *de novo* fat synthetic genes such as, *ACACA*, *FASN*, *SCD*, *ELOVL2*, *CPT1* have been studied. The *ACACA*, *FASN*, *SCD* and *CPT1* genes were down-regulated and *ELOVL2* gene was significantly up-regulated. The fold change of *ACACA*, *FASN*, *SCD*, *CPT1* and *ELOVL2* was 0.55, 0.08, 0.01, 0.05 and 2.87 respectively (Fig. 4).

Quantification of cholesterol and triglycerides

The cholesterol and triglycerides were estimated from the control and *ACACB* knockdown cell lysate and estimated by using Turbo Chem 100 automatic blood analyzer. We found significant ($P < 0.01$) reduction in cholesterol and triglyceride levels in *ACACB* knockdown cells at 47.71% and 34.91% respectively as compared to the control (Fig. 5).

Discussion

Synthesis of potential shRNAs

The success of RNAi depends on the designing of the shRNA for specific target recognition and minimization of off-target effects. In the present study, unique/specific shRNA molecules were designed based on the Reynolds ranking criteria for the *ACACB* gene and also, the specificity of the shRNA sequences is important for the formation of RISC (Reynolds et al. 2004; Paddison et al. 2004). In addition to specificity, the G-C content plays an enormous role in the formation of duplex siRNA molecule. Low G-C content is known to decrease affinity for the target sequence, whereas higher G-C content interferes with RISC formation that eventually cleaves the mRNA molecules. The G-C content of the designed shRNA molecules in the present study was moderate for the duplex siRNA formation. In addition to the G-C content, the lack of internal repeats, an A/U-rich 5' end, Tuschl motifs, and other features were included which improves the silencing efficiency of siRNA (Fuchs et al. 2004). Finally, a simple local alignment search tool (BLAST) was also employed to ensure that shRNA had no significant homologies with genes other than the target to avoid possible off-target effects. Further, silencing performance was also positively associated with the siRNA-mRNA duplex (G_{duplex}) stability (Pascut et al. 2015). Similarly, 1 and 5 shRNAs had higher G_{duplex} values than shRNA 2, 3, and 4 (which had a low G_{duplex} value), meaning that 1 and 5 shRNAs could bind the target site more efficiently. The knockdown efficiency of 1 and 5 shRNAs was high, supporting the above predictions. The duplex asymmetry (DSSE) and target site accessibility could improve knockdown efficiency by about 26% and 40%, respectively (Shao et al. 2007). For enhanced RNAi potency, the siRNAs suitable disruption energy and DSSE is < -10 kcal/mol and > 0.0 kcal/mol, respectively (Shao et al. 2007). We noticed that the expected disruption energies and DSSE for all of the modeled shRNAs were less than -10 kcal/mol and greater than 0.0 kcal/mol, respectively, suggesting that all shRNAs have the ability to silence genes. It has been discovered that the development of self-structures in shRNA (both unimolecular and bimolecular shRNA folding) reduces the equilibrium affinity for the target mRNA (Lu and Mathews, 2007). For all of the shRNAs the predicted self-structure energies in this sample were low, indicating their efficiency in silencing.

Gene silencing caused by shRNAs is mostly due to sequence-specific mRNA degradation by antisense/guide strand of shRNA (Martinez et al. 2002). The 'guide strand' is inserted into the active RNA-induced silencing complex (RISC) to locate the mRNA, which has a complementary sequence leading to the endonucleolytic cleavage of the target mRNA leading to gene silencing (Hannon, 2002). The degree of secondary structure in the antisense strand was of utmost importance in determining the highly active shRNAs among the several factors controlling the efficiency of gene silencing (Patzel et al. 2005). The development of secondary structure in the antisense strand is a significant factor in shRNA-induced gene silencing (Wolfman et al. 2003; Qiao et al. 2008). The guide-RNA structures are categorized as those, greatest silencing caused by sequences that do not form secondary structures, second best are stem-loop structures with ≥ 2 free nucleotides at 5 'end and ≥ 4 free 3' nucleotides, followed by internal-loop, two stem-loop, and short free end stem-loop structures (Patzel et al. 2005). Therefore, it is understood that secondary structure formation correlates negatively with the efficient silencing of the gene. Hairpin-structured shRNAs are unable to fully open during their function, resulting in low gene silencing efficiency. As a result, the RISC-siRNA complex formed would not be that much effective while interacting with the complementary mRNA. The mRNA local structure is one of the key factors with a strong effect on silencing of the shRNA molecule (Schubert et al. 2005; Gredell et al. 2008;

Overhoff et al. 2005; Pascut et al. 2015; Holen 2005; Matveeva et al. 2007). The mRNA contains loop structures that provide easy access to the guide strand for binding the target region which enhances the gene silencing efficiency but the presence of paired nucleotides and hairpins reduced the gene silencing, respectively (Schubert et al. 2005; Holen 2005; Li and Cha 2007). The GC content of the mRNA target region plays a crucial role in loading shRNA into RISC complex (Reynolds et al. 2004; Shah et al. 2007; Wang and Mu 2004; Kretschmer-Kazemi Far 2003; Bohula et al. 2003; Stewart et al. 2008; Luo and Chang 2004). In our study, all the *ACACB* mRNA target regions of shRNAs revealed stem-loop structures and optimum GC% content (42.86 to 47.6). However, there might be some other factors which also contributes to the different silencing efficiency of shRNA constructs.

Following these findings, shRNA constructs 1 and 5 were devoid of any secondary structures in their antisense strands while shRNA constructs 2, 3, and 4 formed secondary structures. Accordingly, shRNA 1 and 5 had higher knockdown efficiency (67 and 69%) respectively, while shRNA 2, 3, and 4 had lower knockdown percentages (25–39%) which confirms the earlier reports (Patzel et al. 2005; Wolfman *et al*. 2003; Qiao et al. 2008). As compared to the control, all the shRNAs showed lower expression of the *ACACB* gene and among the five shRNAs, the shRNA 5 showed higher knockdown whereas shRNA 2 showed lower knockdown respectively.

ACACB gene silencing in chicken myoblast cells

Transfection of shRNA constructs into the CEM resulted in a notable down-regulation of *ACACB* mRNA, implying that CEM culture can be used as an *in vitro* model for some functional studies. Owing to the lack of secondary structures, shRNA 1 and 5 had a higher silencing efficiency than the other shRNAs. In the case of shRNA 2, intrinsic factors such as low duplex energy and high disruption energy may have made the mRNA-shRNA hybridization complex less stable, resulting in incomplete accessibility of the target mRNA region. Secondary structure formation in shRNA 2, 3, and 4 might have reduced their efficiency of silencing by influencing the hybridization of the siRNA/RISC to its target site (Schubert et al. 2005).

In goat fibroblast cells, observed that substantial silencing of *ACTRIIB* gene as 33–66 % (Patel et al. 2014). Besides, several researchers have carried out knockdown experiments on the *MSTN* gene in different animals, including chicken. However, the *MSTN* gene was silenced up to 68 and 75% in chicken embryo fibroblast cells (Sato et al. 2006; Tripathi et al. 2013). Later on, in the same chicken embryo fibroblast cells shRNA was used against *MSTN*, *ACTRIIA*, and *ACTRIIB* genes and observed the knockdown percentage of 68, 82 and 87, respectively (Tripathi et al. 2013; Satheesh et al. 2016; Guru Vishnu et al. 2019). Even in *in vivo* studies, *MSTN* knockdown chicken showed 28% more body weight during 42 days of age compared to the control broiler chicken (Bhattacharya et al. 2017). In duck embryonic fibroblasts, different lentivirus-mediated shRNA groups were compared and showed decreased the *MSTN* mRNA expression by 61.6, 76.9, and 79.1%, respectively (Tao et al. 2015). Further, in caprine foetal fibroblasts, transient transfection of anti-myostatin shRNA decreased the mRNA level by 89 and 72%, respectively (Kumar et al. 2014; Jain et al. 2015). The importance of using thermodynamic features in shRNA designing was highlighted by observing the relationship between shRNA thermodynamic parameters and the silencing performance of different shRNAs. Based on the findings, it is hypothesized that every designed shRNA with $G_{overall}$, G_{duplex}, $G_{breaktarget}$, and G_{ends} of shRNAs in the range of 25 to 32 kcal/mol, 31 to 35 kcal/mol, 1.0 to 1.9 kcal/mol, and > 0.0 Kcal/mol kcal/mol, respectively, would appease for maximum silencing efficiency.

Effect on immune response genes

Although RNA interference has promised to be a powerful experimental tool to manipulate gene function, there has been a growing concern about the use of shRNA due to off-target effects such as activation of immune response. Few studies have stated that both non-immune cells and immune cells can recognize shRNAs independent of the sequence leading to interferon (IFN) induction and inflammatory cytokines both *in vivo* and *in vitro* (Sledz et al. 2003; Judge et al. 2005). The IFN response caused by the activation of dsRNA-dependent protein kinase R (PKR) leads to the global inhibition of protein synthesis (Judge et al. 2005). The dsRNA (> 23-bp) can affect cell viability and induce a powerful interferon response (strong up-regulation of the dsRNA receptor, Toll-like receptor 3) in a cell type-specific manner (Reynolds et al. 2006). It was concluded that the length threshold of siRNA-induced interferon response was not constant, but it differed between various types of cells significantly.

However, shRNAs shorter than 30 bp can evade PKR activation (Robbins et al. 2006) and some experiments exhibited a significant increase in the expression of immune response genes including Scramble shRNA. It was also observed that activation of interferon response in goat myoblast cells due to exogenous administration of shRNA against the *ACTRIIB* gene (Patel et al. 2014). Interferon modulation in chicken embryonic myoblast cells varied between 46–112 folds of OAS1 and 2-7.2 folds for IFNβ compared to mock-transfected control due to anti myostatin shRNA (Tripathi et al. 2013). It has been reported that the shRNA-mediated myostatin knockdown in transgenic sheep showed increased *MHCI* expression (Hu et al. 2013).

There are several reports regarding shRNA-induced interferon responses suggested that a high level of shRNA expression might be due to the accumulation of unprocessed or aberrantly processed transcripts triggering interferon response (Stewart et al. 2008; Cao et al. 2005; Watanabe et al. 2006). The shRNA transfected porcine embryo cells, showed induction of the *OAS1* and IFNβ genes by 1000 and 50 folds respectively (Stewart et al. 2008). Further, reported that the introduction of H1 and U6 promoter-based shRNA constructs by pronuclear microinjection led to induction of *OAS1* gene and early embryo lethality (Bridge et al. 2003). In the present experiment, the expression of interferon genes *IFN α, IFN β*, and *BLB1* were analyzed in control (scrambled shRNA treatment) and knockdown cells possessing different shRNA molecules to explore the impact of shRNA on immune function. It was observed that there was no significant difference of expression of *IFN α, IFN β, BLB1* genes between knockdown and scrambled shRNA treated cells. Hence, shRNA molecules used in the present study have not been captured by the interferon mechanism *in vitro* as any foreign DNA fragment of a specific length is normally detected and destroyed by the interferons. It may therefore be construed that these shRNA molecules have been very much effective to silence *ACACB* expression without interfering with the body's immune system. However, the introduction of short (< 30 nt) dsRNAs with 2-base 3 overhangs resembling dicer processing does not activate the interferon pathway and also shRNA expression from vectors in the nucleus resemble endogenous miRNA (Elbashir et al. 2001). The administration of naked, synthetic siRNAs in mice showed down-regulation of endogenous or exogenous targets without inducing an interferon response (Heidel et al. 2004). Similarly, the *in vitro* siRNA study showed the absence of IFN induction in human CD34 + progenitor cells (Robbins et al. 2006). On the contrary, activation of PKR, OAS, RIG-1, TLR 7, and TLR 8 by sequences shorter than 19 bp (Gantier et al. 2007).

Effect of *ACACB* gene silencing on *de novo* fat synthetic genes

Now-a-days, researchers are more focused on *ACACA* and *ACACB* to understand the chemistry and biological activity because they are very important enzymes in fatty acid synthesis and oxidation. The *ACACB* gene is localized subcellularly on the mitochondrial membrane and is involved in the synthesis of malonyl-CoA, and this inhibits the *CPT1*, which plays an important role for controlling the two opposing pathways i.e. fatty acid synthesis and oxidation. In this study, we knocked down the *ACACB* gene in chicken myoblast cells and tracked the expression of key fatty acid metabolism genes such as *ACACA*, *FASN*, *SCD*, *ELOVL2*, and *CPT1*. We observed down-regulation of *ACACA*, *FASN*, *SCD*, and *CPT1* gene and up-regulation of *ELOVL2* in *ACACB* knockdown myoblast cells. The down-regulation of *ACACA*, *FASN*, *SCD* genes indicates suppression of the fatty acid synthesis, and up-regulation of *ELOVL2* indicates the enhancement of long-chain fatty acids formation (Fig. 6). The *CPT1* is a rate-limiting enzyme and down-regulation of this enzyme indicates blocking the β-oxidation for balancing the fatty acid synthesis and oxidation because of fewer fats accumulation in the tissues.

Effect of *ACACB* gene silencing on cholesterol and triglyceride synthesis

In chicken egg and meat the high cholesterol and triglycerides are most undesired components and which compels us to eat chicken products in less quantity. The *ACVR2B* knockdown chicken showed significantly low cholesterol (Bhattacharya et al. 2019). In mice, LNP-formulated siRNAs were used for knockdown of the ApoB gene resulted in significant reduction of total cholesterol and LDL cholesterol, which suggested that targeting ApoB is a therapeutic approach for hyperlipidaemia treatment (Tadin-Strapps et al. 2011). In this study, we observed a significant reduction of cholesterol and triglycerides at 47.71% and 34.91%, respectively in *ACACB* knockdown cell lysate compared to the control. Based on these results, we suggest that the *ACACB* knockdown chicken may produce low cholesterol and triglycerides.

In conclusion, from the present study we have identified potential shRNA molecules against the *ACACB* gene where shRNA1 and shRNA5 showed more than 60% knockdown efficiency on the expression of the *ACACB* gene under *in vitro* myoblast cell culture system. The silencing of the *ACACB* gene showed to have a direct effect on the down-regulation of *ACACA*, *FASN*, *SCD*, and *CPT1* genes, and up-regulation of *ELOVL2* gene in myoblast cells. We suggest that these shRNA molecules may be used under *in vivo* system for the development of knockdown chicken having a potential of producing lean meat by silencing of expression of the *ACACB* gene.

Declarations

Acknowledgements The authors duly acknowledge the funding support by the ICAR, Govt. of India under National Fellow project for conducting this experiment. The work has been the PhD Dissertation work of the first author. The authors also extend thanks to the Director, ICAR-Directorate of Poultry Research, Hyderabad for providing support to conduct animal experiment and other facilities. Authors also thank to the Dean, College of Veterinary Science, PVNRTVU, Hyderabad for providing necessary supports for conducting the experiments.

Authors' Contributions G. S conducted the wet lab experiments and prepared the first draft. P. J. L carried out the statistical analysis. S. T. V. R prepared all the tables. R. M. V. P prepared all the figures. M. K edited the draft. C. S. P and A. R. P helped in cell culture. D. D helped in wet lab experiments. T. K. B conceived the idea, prepared the plan of work and final editing of the draft.

Funding The results presented here were funded by the ICAR, Govt. of India under National Fellow project.

Compliance with ethical standards

The entire study was approved by the Institute Animal Ethics committee (IAEC) and Institute Bio-safety Committee (IBSC) of ICAR-Directorate of Poultry Research, Hyderabad, India. All the bio-safety guidelines of IBSC were followed while conducting the experiments.

Conflict of interest The authors have no conflict of interest.

References

1. Abu-Elheiga L, Brinkley WR, Zhong L, Chirala SS, Woldegiorgis G, Wakil SJ (2000) The subcellular localization of acetyl-CoA carboxylase 2. Proc Natl Acad Sci USA 97(4):1444–1449. https://doi.org/10.1073/pnas.97.4.1444
2. Abu-Elheiga L, Matzuk MM, Abo-Hashema KAH, Wakil SJ (2001) Continuous fatty acid oxidation and reduced fat storage in mice lacking acetyl-CoA carboxylase 2. Science 291(5513):2613–2616. https://doi.org/10.1126/science.1056843
3. Abu-Elheiga L, Oh W, Kordari P, Wakil SJ (2003) Acetyl-CoA carboxylase 2 mutant mice are protected against obesity and diabetes induced by high-fat/high-carbohydrate diets. Proc Natl Acad Sci USA 100(18):10207–10212. https://doi.org/10.1073/pnas.1733877100
4. Abu-Elheiga L, Matzuk MM, Kordari P, Oh WK, Shaikenov T, Gu Z, Wakil SJ (2005) Mutant mice lacking acetyl-CoA carboxylase 1 are embryonically lethal. Proc Natl Acad Sci USA 102(34):12011–12016. https://doi.org/10.1073/pnas.0505714102
5. Becker WA, Spencer JV, Mirosh LW, Verstrate JA (1979) Prediction of Fat and Fat Free Live Weight in Broiler Chickens Using Back skin Fat Abdominal Fat and Live Body Weight. Poult Sci 58(4):835–842. https://doi.org/10.3382/ps.0580835
6. Bhattacharya TK, Shukla R, Chatterjee RN, Bhanja SK (2019) Comparative analysis of silencing expression of myostatin (*MSTN*) and its two receptors (ACVR2A and ACVR2B) genes affecting growth traits in knockdown chicken. Sci Rep 9:7789. https://doi.org/10.1038/s41598-019-44217-z
7. Bhattacharya TK, Shukla R, Chatterjee RN, Dushyanth K (2017) Knockdown of the myostatin gene by RNA interference increased body weight in chicken. J Biotechnol 241:61–68. https://doi.org/10.1016/j.jbiotec.2016.11.012

8. Bohula EA, Salisbury AJ, Sohail M, Playford MP, Riedemann J, Southern EM, Macaulay VM (2003) The efficacy of small interfering RNAs targeted to the type 1 insulin like growth factor receptor (IGF1R) is influenced by secondary structure in the IGF1R transcript. J Biol Chem 278(18):15991–15997. https://doi.org/10.1074/jbc.M300714200
9. Bridge AJ, Pebernard S, Ducraux A, Nicoulaz AL, Iggo R (2003) Induction of an interferon response by RNAi vectors in mammalian cells. Nat Genet 34(3):263–264. https://doi.org/10.1038/ng1173
10. Butterwith SC (1989) Contribution of lipoprotein lipase activity to the differential growth of three adipose tissue depots in young broiler chickens. Br Poult Sci 30(4):927–933. https://doi.org/10.1080/00071668908417219
11. Buys N, Buyse J, Hassanzadeh-Ladmakhi M, Decuypere E (1998) Intermittent Lighting Reduces the Incidence of Ascites in Broilers: An Interaction with Protein Content of Feed on Performance and the Endocrine System. Poult Sci 77(1):54–61. https://doi.org/10.1093/ps/77.1.54
12. Buyse J, Leenstra FR, Zeman M, Rahimi G, Decuypere E (1999) A comparative study of different selection strategies to breed leaner meat-type poultry. Poult Avian Biol Rev 10(3):121–142
13. Cable MC, Waldroup PW (1990) Effect of different nutrient-restriction programs early in life on broiler performance and abdominal fat content. Poult Sci 69(4):652–660. https://doi.org/10.3382/ps.0690652
14. Cahaner A, Nitsan Z, Nir I (1986) Weight and Fat Content of Adipose and Nonadipose Tissues in Broilers Selected For or Against Abdominal Adipose Tissue. Poult Sci 65(2):215–222. https://doi.org/10.3382/ps.0650215
15. Cao W, Hunter R, Strnatka D, McQueen CA, Erickson RP (2005) DNA constructs designed to produce short hairpin interfering RNAs in transgenic mice sometimes show early lethality and an interferon response. J Appl Genet 46(2):217–225
16. Crespo N, Esteve-Garcia E (2002) Dietary polyunsaturated fatty acids decrease fat deposition in separable fat depots but not in the remainder carcass. Poult Sci 81(4):512–518. https://doi.org/10.1093/ps/81.4.512
17. Dunnington EA, Siegel PB, Cherry JA, Jones DA, Zelenka DJ (1986) Physiological traits in adult female chickens after selection and relaxation of selection for 8-week body weight. Zeitschriftfüer Tierzüchtung Zuchtungsbiologie 10(3):51–58. https://doi.org/10.1111/j.1439-0388.1986.tb00066.x
18. Elbashir SM, Lendeckel W, Tuschl T (2001) RNA interference is mediated by 21- and 22-nucleotide RNAs. Genes Dev 15(2):188–200. https://doi.org/10.1101/gad.862301
19. Fuchs U, Damm-welk C, Borkhardt A (2004) Silencing of disease-related genes by small interfering RNAs. Curr Mol Med 4(5):507–517. https://doi.org/10.2174/1566524043360492
20. Gantier MP, Williams BRG (2007) The response of mammalian cells to double-stranded RNA. Cytokine Growth Factor Rev 185(5–6):363–371. https://doi.org/10.1016/j.cytogfr.2007.06.016
21. Gredell JA, Berger AK, Walton SP (2008) Impact of target mRNA structure on siRNA silencing efficiency: a large-scale study. Biotechnol Bioeng 100(4):744–755. https://doi.org/10.1002/bit.21798
22. Griffin HD (1996) Understanding genetic variation in fatness in chickens. Annual report Edinburgh Roslin Institute 95(96):35–38
23. Guru Vishnu P, Bhattacharya TK, Bhushan B, Kumar P, Chatterjee RN, Paswan C, Dushyanth K, Divya D, Prasad AR (2019) In silico prediction of short hairpin RNA and *in vitro* silencing of activin receptor type IIB in chicken embryo fibroblasts by RNA interference. Mol Biol Rep 46(3):2947–2959. https://doi.org/10.1007/s11033-019-04756-0
24. Hannon GJ (2002) RNA interference. Nature 418(6894):244–251. https://doi.org/10.1038/418244a
25. Haro CV (2005) Interaction between dietary polyunsaturated fatty acids and vitamin E in body lipid composition and alfa-tocopherol content of broiler chickens. Thesis PhD. University at Autonoma de Barcelona Spain 140 p
26. Havenstein GB, Ferket PR, Qureshi MA (2003) Growth livability and feed conversion of 1957 versus 2001 broilers when fed representative 1957 and 2001 broiler diets. Poult Sci 82(10):1500–1508. https://doi.org/10.1093/ps/82.10.1500
27. Heidel JD, Hu S, Liu XF, Triche TJ, Davis ME (2004) Lack of interferon response in animals to naked SiRNAs. Nat Biotechnol 22(12):1579–1582. https://doi.10.1038/nbt1038

28. Hemann MT, Fridman JS, Zilfou JT, Hernando E, Paddison PJ, Cordon-Cardo C, Hannon GJ, Lowe SW (2003) An epi-allelic series of p53 hypomorphs created by stable RNAi produces distinct tumor phenotypes *in vivo*. Nat Genet 33(3):396–400. https://doi.org/10.1038/ng1091
29. Holen T (2005) Mechanisms of RNAi: mRNA cleavage fragments may indicate stalled RISC. Journal of RNAi gene silencing: an international journal of RNA gene targeting research 1(1):21
30. Hu S, Ni W, Sai W, Zi H, Qiao J, Wang P, Sheng J, Chen C (2013) Knockdown of Myostatin Expression by RNAi Enhances Muscle Growth in Transgenic Sheep. PLoS One 8(3):e58521. https://doi.org/10.1371/journal.pone.0058521
31. Jain SK, Jain H, Kumar D, Bedekar MK, Pandey AK, Sarkhel BC (2015) Quantitative Evaluation of Myostatin Gene in Stably Transfected Caprine Fibroblast Cells by Anti-Myostatin shRNA. Appl Biochem Biotechnol 177(2):486–497. https://doi.org/10.1007/s12010-015-1757-1
32. Jennen DGJ (2004) Chicken fatness from QTL to candidate gene. Thesis PhD Wageningen University. The Netherlands 176 p
33. Judge AD, Sood V, Shaw JR, Fang D, McClintock K, MacLachlan I (2005) Sequence dependent stimulatnion of the mammalian innate immune response by synthetic siRNA. Nat Biotechnol 23(4):457–462. https://doi.org/10.1038/nbt1081
34. Kretschmer-Kazemi Far R, Sczakiel G (2003) The activity of siRNA in mammalian cells is related to structural target accessibility: a comparison with antisense oligonucleotides. Nucleic Acids Res 31(15):4417-24. https://doi.10.1093/nar/gkg649
35. Kumar R, Singh SP, Kumari P, Mitra A (2014) Small interfering RNA siRNA-mediated knockdown of myostatin influences the expression of myogenic regulatory factors in caprine foetal myoblasts. Appl Biochem Biotechnol 172(3):1714–1724. https://doi.org/10.1007/s12010-013-0582-7
36. Leenstra FR (1986) Effect of age sex genotype and environment on fat deposition in broiler chickens—A review. World's Poult Sci J 42(1):12–25. https://doi.org/10.1079/WPS19860002
37. Leeson S, Summers JD (1980) Production and Carcass Characteristics of the Broiler Chicken. Poult Sci 59(4):786–798. https://doi.org/10.3382/ps.0590786
38. Li W, Cha L (2007) Predicting siRNA efficiency. Cell Mol Life Sci CMLS 64(14):1785–1792. https://doi.org/10.1007/s00018-007-7057-3
39. Lippens M (2003) The influence of feed control on the growth pattern and production parameters of broiler chicken. Thesis PhD Ghent University Belgium 203p
40. Lu ZJ, Mathews DH (2007) Efficient siRNA selection using hybridization thermodynamics. Nucleic Acids Res 36(2):640–647. https:// doi.org:10.1093/nar/gkm920
41. Luo KQ, Chang DC (2004) The gene-silencing efficiency of siRNA is strongly dependent on the local structure of mRNA at the targeted region. Biochem Biophys Res Commun 318(1):303–310. https://doi.org/10.1016/j.bbrc.2004.04.027
42. Martinez J, Patkaniowska A, Urlaub H, Lührmann R, Tuschl T (2002) Single stranded antisense siRNAs guide target RNA cleavage in RNAi. Cell 110(5):563–574. https://doi.org/10.1146/annurev.genom.8.080706.092424
43. Matveeva O, Nechipurenko Y, Rossi L, Moore B, Sætrom P, Ogurtsov AY, Atkins JF, Shabalina SA (2007) Comparison of approaches for rational siRNA design leading to a new efficient and transparent method. Nucleic Acids Res 35(8):e63. https://doi.org/10.1093/nar/gkm088
44. Nikolova N, Pavlovski Z, Milosevic N, Peric L (2007) The quantity of abdominal fat in broiler chicken of different genotypes from fifth to seventh week of age. Biotechnology in Animal Husbandry Biotehnologija u Stocarstvu 23(5-6-2):331–338. https://doi.org/10.2298/BAH0702331N
45. Oh SY, Lee MY, Kim JM, Yoon S, Shin S, Park YN, Ahn YH, Kim KS (2005) Alternative usages of multiple promoters of the acetyl-CoA carboxylase beta gene are related to differential transcriptional regulation in human and rodent tissues. J Biol Chem 280:5909–5916. https://doi.org/10.1074/jbc.M409037200

46. Overhoff M, Alken M, Far RK, Lemaitre M, Lebleu B, Sczakiel G, Robbins I (2005) Local RNA target structure influences siRNA efficacy: a systematic global analysis. J Mol Biol 348(4):871–881. https://doi.org/10.1016/j.jmb.2005.03.012
47. Paddison PJ, Caudy AA, Bernstein E, Hannon GJ, Conklin DS (2002) Short hairpin RNAs shRNAs induce sequence-specific silencing in mammalian cells. Genes Dev 16(8):948–958. https://doi.org/10.1101/gad.981002
48. Pascut D, Bedogni G, Tiribelli C (2015) Silencing efficacy prediction: a retrospective study on target mRNA features. Biosci Rep 35(2):e00185. https://doi.org/10.1042/BSR20140147
49. Patel AK, Tripathi AK, Patel UA, Shah RK, Joshi CG (2014) Myostatin knockdown and its effect on myogenic gene expression program in stably transfected goat myoblasts. *In vitro* Cell Dev Biol Animal 50(7):587–596. https://doi.org/10.1007/s11626-014-9743-4
50. Patzel V, Rutz S, Dietrich I, Köberle C, Scheffold A, Kaufmann SHE (2005) Design of siRNAs producing unstructured guide-RNAs results in improved RNA interference efficiency. Nat Biotechnol 23(11):1440–1444. https://doi.org/10.1038/nbt1151
51. Pym RAE (1987) Techniques to reduce adiposity in meat chickens. Proc Nutr Soc Aust 12:46–55
52. Qiao J, Moreno J, Sanchez-Perez L, Kottke T, Thompson J, Caruso M, Diaz RM, Vile R (2006) VSV-G pseudotyped, MuLV-based, semi-replication-competent retrovirus for cancer treatment. Gene Ther 13(20):1457–1470. https://doi.org/10.1038/sj.gt.3302782
53. Reynolds A, Anderson EM, Vermeulen A, Fedorov Y, Robinson K, Leake D, Karpilow J, Marshall WS, Khvorova A (2006) Induction of the interferon response by siRNA is cell type- and duplex length-dependent. RNA 12(6):988–993. https://doi.org/10.1261/rna.2340906
54. Reynolds A, Leake D, Boese Q, Scaringe S, Marshall WS, Khvorova A (2004) Rational siRNA design for RNA interference. Nat Biotechnol 22(3):326–330. https://doi.org/10.1038/nbt936
55. Robbins MA, Li M, Leung I, Li H, Boyer DV, Song Y, Behlke MA, Rossi JJ (2006) Stable expression of shRNAs in human CD34 + progenitor cells can avoid induction of interferon responses to siRNAs *in vitro*. Nat Biotechnol 24(5):566–571. https://doi.org/10.1038/nbt1206
56. Saadoun A, Leclercq B (1986) *In vivo* lipogenesis in genetically fat and lean chickens of various ages. Comp Biochem Physiol B Comp Biochem 83(3):607–611. https://doi.org/10.1016/0305-0491(86)90304-4
57. Satheesh P, Bhattacharya TK, Kumar P, Chatterjee RN, Dhara SK, Paswan C, Shukla R, Dushyanth K (2016) Gene expression and silencing of activin receptor type 2A ACVR2A in myoblast cells of chicken. Br Poult Sci 57(6):763–770. https://doi.org/10.1080/00071668.2016.1219693
58. Sato F, Kurokawa M, Yamauchi N, Hattori M (2006) Gene silencing of myostatin in differentiation of chicken embryonic myoblasts by small interfering RNA. Am J Physiol Cell Physiol 291(3):C538–C545. https://doi.org/10.1152/ajpcell.00543.2005
59. Schubert S, Grünweller A, Erdmann VA, Kurreck J (2005) Local RNA target structure influences siRNA efficacy: systematic analysis of intentionally designed binding regions. J Mol Biol 348(4):883–893. https://doi.org/10.1016/j.jmb.2005.03.011
60. Shah JK, Garner HR, White MA, Shames DS, Minna JD (2007) sIR: siRNA Information Resource, a web-based tool for siRNA sequence design and analysis and an open access siRNA database. BMC Bioinformatics 8(1):178. https://doi.org/10.1186/1471-2105-8-178
61. Shao Y, Chan CY, Maliyekkel A, Lawrence CE, Roninson IB, Ding Y (2007) Effect of target secondary structure on RNAi efficiency. RNA 13(10):1631–1640. https://doi.org/10.1261/rna.546207
62. Sledz CA, Holko M, De Veer MJ, Silverman RH, Williams BRG (2003) Activation of the interferon system by short-interfering RNAs. Nat Cell Biol 5(9):834–839. https://doi.org/10.1038/ncb1038
63. Stewart CK, Li J, Golovan SP (2008) Adverse effects induced by short hairpin RNA expression in porcine fetal fibroblast. Biochem Biophys Res Commun 370(1):113–117. https://doi.org/10.1016/j.bbrc.2008.03.041
64. Tadin-Strapps M et al (2011) siRNA-induced liver ApoB knockdown lowers serum LDL-cholesterol in a mouse model with human-like serum lipids. J Lipid Res 52(6):1084–1097. https://doi.org/10.1194/jlr.M012872

65. Tao Z, Zhu C, Song C, Song W, Ji G, Shan Y, Xu W, Li H (2015) Lentivirus-mediated RNA interference of myostatin gene affects MyoD and Myf5 gene expression in duck embryonic myoblasts. Br Poult Sci 56(5):551–558. https://doi.org/10.1080/00071668.2015.1085958
66. Thomas VG, Mainguy SK, Prevett JP (1983) Predicting fat-content of geese from abdominal fat weight. J Wildl Manage 47(4):1115–1119. https://doi.org/10.2307/3808172
67. Tripathi AK, Aparnathi MK, Vyavahare SS, Ramani UV, Rank DN, Joshi CG (2012) Myostatin gene silencing by RNA interference in chicken embryo fibroblast cells. J Biotechnol 160(3–4):140–145. https://doi.org/10.1016/j.jbiotec.2012.03.001
68. Tripathi AK, Aparnathi MK, Patel AK, Joshi CG (2013) *In vitro* silencing of myostatin gene by shRNAs in chicken embryonic myoblast cells. Biotechnol Prog 29(2):425–431. https://doi.org/10.1002/btpr.1681
69. Wang L, Mu FY (2004) A Web-based design center for vector-based siRNA and siRNA cassette. Bioinformatics 20(11):1818–1820. https://doi.org/10.1093/bioinformatics/bth164
70. Wang PY, Jiang JJ, Li N, Sheng JL, Ren Y (2010) Transgenic mouse model integrating siRNA targeting the foot and mouth disease virus. Antivir Res 87(2):265–268. https://doi.org/10.1016/j.antiviral.2010.02.319
71. Watanabe T, Sudoh M, Miyagishi M (2006) Intracellular-diced dsRNA has enhanced efficacy for silencing HCV RNA and overcomes variation in the viral genotype. Gene Ther 13(11):883–892. https://doi.org/10.1038/sj.gt.3302734
72. Wolfman JC, Palmby T, Der CJ, Wolfman A (2002) Cellular N-Ras promotes cell survival by downregulation of Jun N-Terminal protein kinase and p38. Mol Cell Biol 22:1589–1606. https://doi.org/10.1128/mcb.22.5.1589-1606.2002
73. Zubair AK, Leeson S (1996) Compensatory growth in the broiler chicken: A review. World's Poult Sci J 52(2):189–201. https://doi.org/10.1079/WPS19960015

Figures

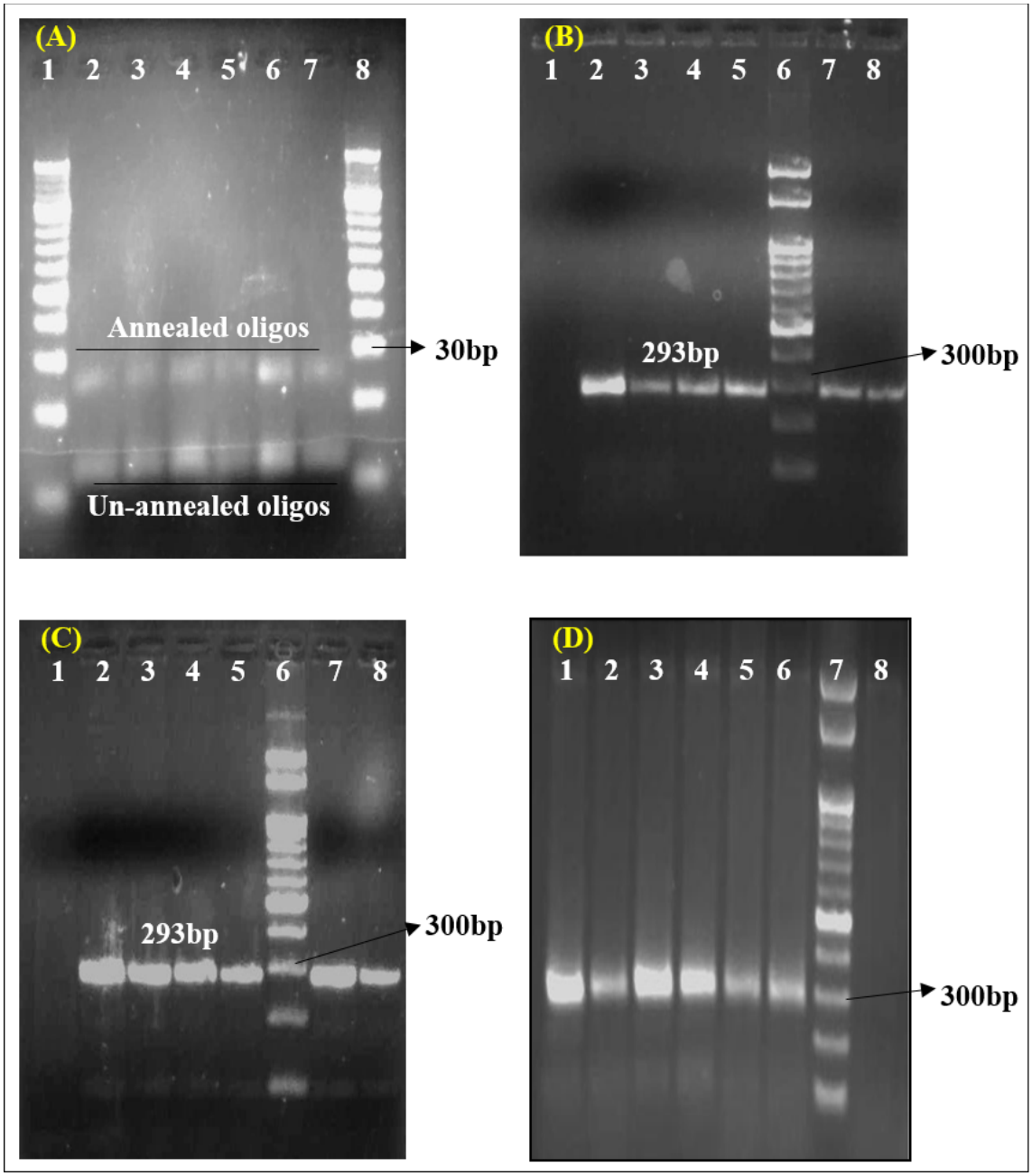

Figure 1

(A) generation of double-stranded oligo (ds oligo). Lane 1 and 8: 20 bp DNA ladder; Lane 2: annealed scrambled oligo; Lane 3-7: annealed shRNA oligos 1-5. (B) and (C) Agarose gel electrophoresis of colony and plasmid PCR amplified fragment (293 bp) of anti ACACB shRNA constructs. Lane 1: negative control; Lane 2-5, 7: anti ACACB shRNA constructs 1-5; Lane 8: Scrambled shRNA construct; Lane 6: 100 bp plus DNA ladder. (D) Agarose gel electrophoresis of DNA from cell lysate amplified fragment (293 bp) of anti ACACB shRNA constructs. Lane 1-5: anti ACACB shRNA constructs; Lane 6: scrambled shRNA construct; Lane 7: 100 bp plus DNA ladder. Lane 8: negative control.

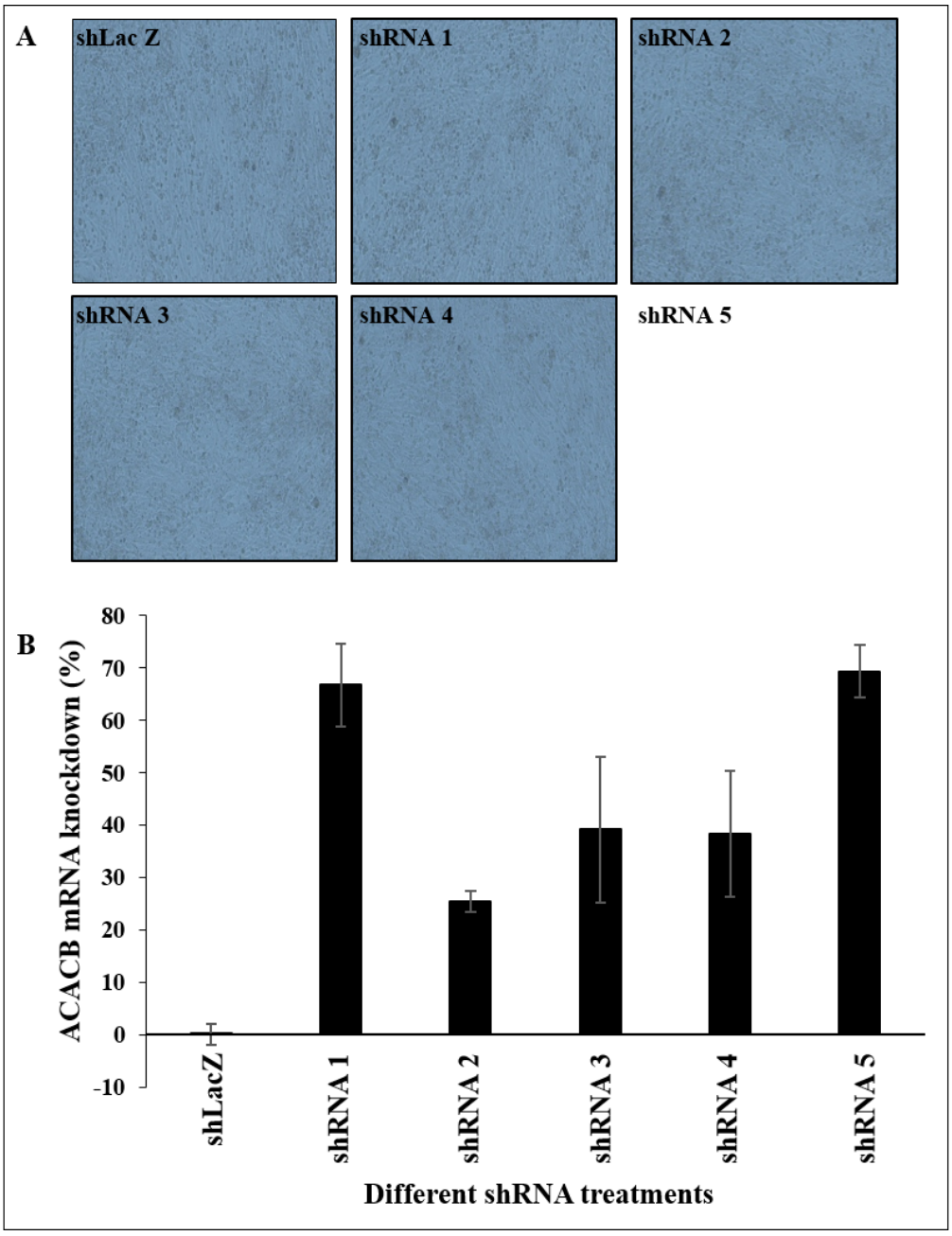

Figure 2

(A) The CEM cells transfected with different shRNA constructs and before harvesting the cells were photographed by using a DeltaPIX microscope. (B) Knockdown efficiency of anti ACACB shRNA constructs in CEM. ShRNA 1-5: Anti ACACB shRNA constructs; shLac Z: negative control (scrambled shRNA).

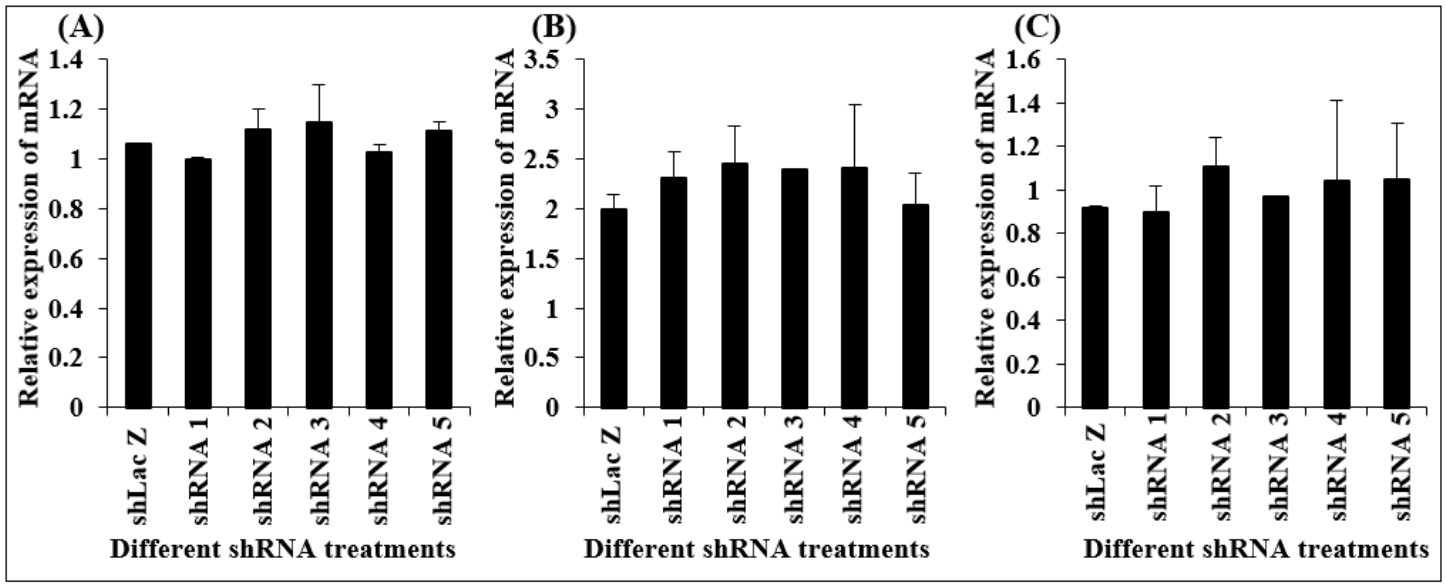

Figure 3

Induction of immune response genes due to anti ACACB shRNA constructs. shRNA 1-5: anti ACACB shRNA constructs, shLacZ: negative control (scrambled shRNA). (A) IFNA: Interferon A; (B) IFNB: Interferon B; (C) BLB1: Major Histocompatibility complex II beta chain BLB1.

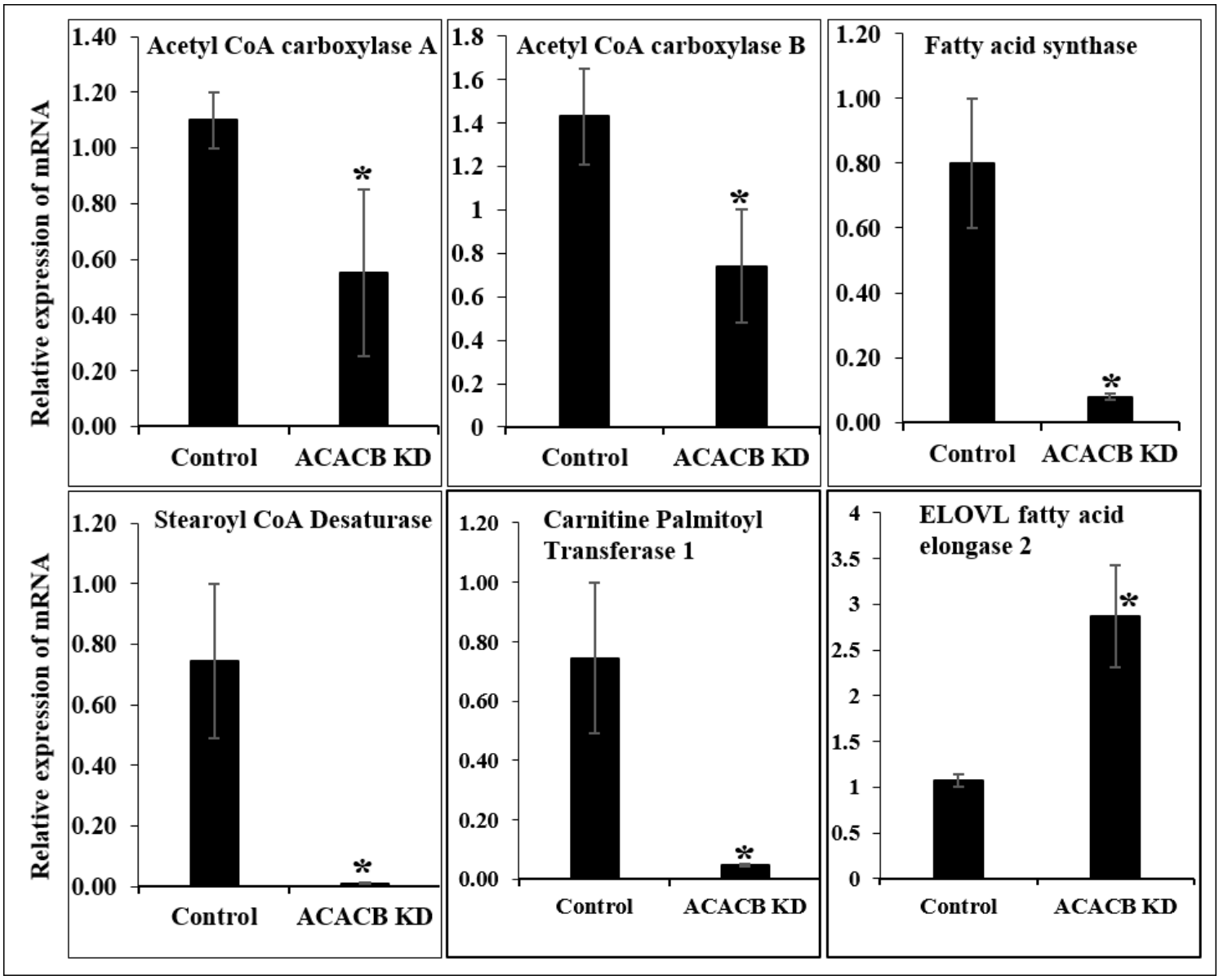

Figure 4

Gene expression associated with fatty acid metabolism related genes in ACACB knockdown chicken myoblast primary cells compared with control cells. Mean values were different at *P ≤ 0.05.

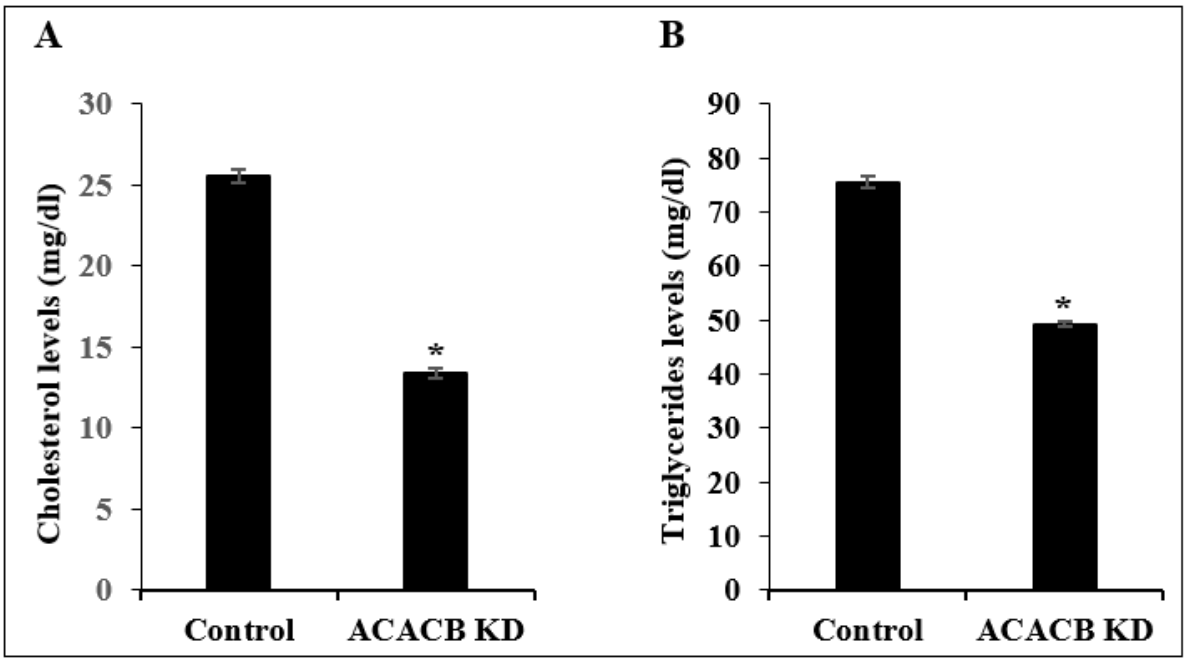

Figure 5

Estimation of cholesterol (A) and triglycerides (B) in ACACB knockdown chicken myoblast primary cells compared with control cells. Mean values were different at *P ≤ 0.01.

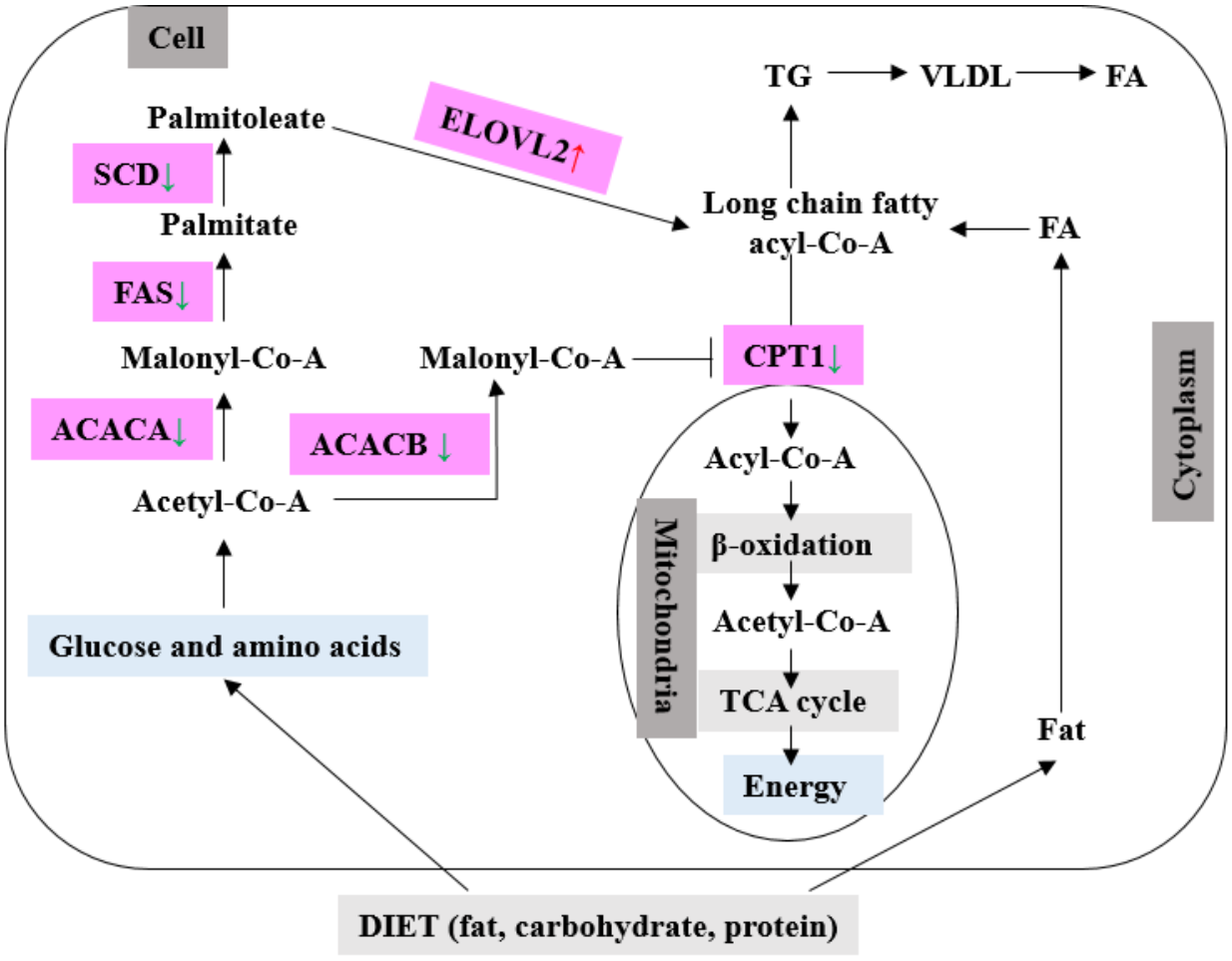

Figure 6

Diagrammatic representation of targeted gene expression analysis conducted in the present study. In chicken tissues, Acetyl-coenzyme A carboxylase 1 (ACACA) and acetyl-coenzyme A carboxylase 2 (ACACB) play distinct roles in lipid metabolism. Diet fat, carbohydrate, and protein are digested, and the fatty acids (FA), glucose, and amino acids are transported to various tissues, including liver, adipose, and muscle. In the cytosol acetyl-CoA is carboxylated to malonyl-CoA by ACC1 and utilized through fatty acid synthase (FAS) and Stearoyl CoA Desaturase (SCD) reactions to generate palmitate and palmitoleate, which is utilized in the synthesis of triglycerides (TG) and VLDL. Also, acetyl-CoA is carboxylated by ACC2 at the mitochondrial membrane to form malonyl-CoA, which inhibits the CPT1 and reduces acyl-CoA transfer to mitochondria for β-oxidation. The down and up arrow (↓) indicates the down and up-regulation of genes in ACACB knockdown CEM primary cells compared to the control cells. Mean values were different at *P ≤ 0.05.

Supplementary Files

This is a list of supplementary files associated with this preprint. Click to download.

- supplementaryFigures.pptx